Solar Energy Materials & Solar Cells 211 (2020) 110508

Contents lists available at ScienceDirect

Solar Energy Materials and Solar Cells

journal homepage: http://www.elsevier.com/locate/solmat

Light and elevated temperature induced degradation in B–Ga co-doped cast mono Si PERC solar cells

Chunlan Zhou [a,b,*], Fangxu Ji [a,b], Shangzhi Cheng [a,b], Junjie Zhu [c], Wenjing Wang [a,b], Dongli Hu [d]

[a] The Key Laboratory of Solar Thermal Energy and Photovoltaic System, Institute of Electrical Engineering, Chinese Academy of Science, Beijing, China
[b] University of Chinese Academy of Sciences, Beijing, China
[c] Solar Energy Department, Institute for Energy Technology, Kjeller, Norway
[d] Jiangsu GCL Silicon Material Technology Development Co., Ltd., Jiang su, China

ARTICLE INFO

Keywords:
Cast mono silicon
Passivated emitter and rear cell (PERC)
Light- and elevated temperature-induced degradation (LeTID)

ABSTRACT

The utilization of boron-doped Si solar cells based on the structure of a passivated emitter and rear cell (PERC) in the solar industry has increased recently. However, this type of high efficiency solar cell is exposed to a so-called light and elevated temperature induced degradation (LeTID). A suppressing of mc-Si LeTID has been studied through a regeneration treatment at high temperature under illumination or in the dark, but most was about the lifetime samples. In this work, to evaluate the applicability of regeneration and annealing at industrial relevant conditions, industrially made B–Ga co-doped cast-mono Si PERC solar cells were treated in a light soaking tool in which the intensity of light and substrate temperature could be adjusted separately and a rapid thermal process (RTP) system. This treatment was evaluated during a subsequent intentional degradation under conditions of 75 °C with an LED white light source at an intensity of 1 kW/m^2. The results showed that properly regenerated samples by high intensity illumination at elevated temperatures suffered from the least degradation, while untreated solar cells had most severe degradation. The RTP method could improve the performance of the solar cells but the RTP-treated samples were less stable than the regenerated samples. It demonstrates the application of a fast (around 20 min) regeneration method could be coupled in mass production. Further, RTP treatment combining with an accelerated regeneration step may be a potential method to provide both the improved performance and high anti-LeTID properties in Si PERC solar cells.

1. Introduction

Today's commercially available, high-efficiency, boron-doped Si solar cells are based on the structure of a passivated emitter and rear cell, or PERC. PERC is a mature technology with a relatively simple manufacturing process and therefore benefits from low cost of ownership. Combining high efficiency and low costs, PERC has started taking off in the solar industry recently. However, this type of high efficiency solar cell is exposed to a so-called degradation process when it is annealed at the end of its fabrication, due to high temperature either combined with high illumination intensity, which is called light and elevated temperature induced degradation (LeTID), or high current density injection in the dark (CID) [1]. Multiple research teams have discovered that mc-Si and Cz-Si PERC solar cells can degrade by more than 10% when exposed to light at temperatures above 50 °C [2,3]. Continued exposure to conditions that induce degradation has been shown to lead to an eventual recovery, or 'regeneration' of minority carrier lifetime. However, this recovery time takes longer than that of conventional full-Al back field (Al-BSF) solar cells; the time may be up to thousands of hours, which can be equal to or exceed the service time in the field, especially for mc-Si PERC solar cells.

LeTID has become a potential limiting factor for the development of P-type crystalline Si high-efficiency PERC solar cells, but until now reported LeTID behaviors have been varied. The degree of LeTID can be strongly influenced by the solar cells' preparation process [4]. Furthermore the light annealing greatly changes the degradation-regeneration process [5]. It was found that dark annealing also changed degradation characteristics [6]. Moreover, it has been

* Corresponding author. The Key Laboratory of Solar Thermal Energy and Photovoltaic System, Institute of Electrical Engineering, Chinese Academy of Science, Beijing, China.
E-mail address: zhouchl@mail.iee.ac.cn (C. Zhou).

https://doi.org/10.1016/j.solmat.2020.110508
Received 20 January 2020; Received in revised form 3 March 2020; Accepted 9 March 2020
Available online 28 March 2020

found that not only the temperature [7], but also the carrier injection level is influenced by operating conditions [2,8] (e.g. open-voltage, short-circuit, and maximum power point) and the illumination intensity evidently changes the LeTID behavior of PERC solar cells [2,9]. These factors lead to large variation in the conditions under which LeTID occurs, so LeTID identified by different researchers may have similar or different origins. Due to the complexity of the factors that produce LeTID, the root causes of the degradation remain unclear to date.

Recently, there have been some results regarding high intensity illumination treatments at elevated temperatures (laser or LED white light source) that accelerate the regeneration of P-type mc-Si [10,11]. Similarly, a forward bias voltage used on the solar cells in the dark at elevated temperatures could suppress LeTID by activating and accelerating the regeneration process [12]. These methods have proven to be effective for passivating BO defects, but may not be as successful on LeTID because of their slow reaction time and the uncertain long-term stability of the regenerated cells. An additional firing step at a reduced temperature after cell metallization could also suppress the extent of V_{oc} degradation [13]. Chandany et al. applied a rapid thermal processing (RTP) pre-fire annealing step at low temperature to effectively suppress LeTID on p-type mc-Si lifetime samples [14]. Furthermore, Koski et al. [15] used annealing in the dark for 18.5 h at 300 °C to eliminate the LeTID behavior in p-type mc-Si lifetime samples. These treatments on lifetime samples present potential methods for suppressing LeTID; however, their feasibility is still in question because the effect of these processes on the solar cells efficiency and the reduction of LeTID is still unknown.

In addition to p-type multi-crystalline and Cz Si PERC solar cells, similar LeTID behavior has been observed in float-zone Si [16], n-type cast-grown multi-crystalline, and p-type mono-like Si [17]. Studies have clearly shown that the degradation of the boron-doped mc-Si PERC solar cell was much more serious than Ga-doped mc-Si PERC solar cells [1], which was ascribed to the more severe BO_x-LID (boron-oxygen complex-induced light induced degradation) found in the boron-doped mc-Si [18]. To the best of our knowledge, no studies have been reported on the LeTID of B–Ga co-doped cast mono Si PERC solar cells. Mono-like Si contains similar amounts of metal impurities as mc-Si, but features a distinct crystallographic structure [19]. Thus, it was hypothesized that the LeTID behavior in cast mono Si solar cells may be similar to mc-Si, not mono Si. In this work, high intensity illumination at elevated temperatures and the RTP method were investigated, and the effects of temperature and time on degradation, regeneration, and the resulting stability were analyzed. We were especially interested in the dissociation and association of the Fe–B pairs and the role they play in the degradation and regeneration cycle during light soaking, since earlier studies indicate that the Fe impurity may still be present in the Si bulk after the last firing step [20] and exists in the form of Fe_i during LeTID [21]. Moreover, whether the RTP treatment could modulate or mitigate the degradation ratio and whether the defect kinetics of light soaking and RTP are similar or not was examined. In order to address these questions, the light soaking accelerated regeneration process was carried out with the maximum light intensity of 7 suns in the temperature range of 150 °C–250 °C on the finished B–Ga co-doped cast-mono Si PERC solar cells. RTP was also conducted on the finished cells at various temperatures (250–450 °C) and durations (1–12 min), which is compatible with the industrial process and can be easily introduced to the production line. All regenerated solar cells were used to test the performance stability under the conditions of LeTID: 75 °C with 1 kW/m^2.

2. Experimental

156.75 mm × 156.75 mm PERC solar cells made of phosphorus compensation B–Ga co-doped cast mono-crystalline Si with a thickness of 180 μm and resistivity of approximately 2 Ω cm were sourced from GCL Energy Holdings. The wafers were selected from the neighboring positions in the ingot (sister wafers) and with interstitial oxygen concentrations of 5 ppma (Group A) and 7 ppma (Group B), with B, Ga, and P concentrations of 1.17×10^{16}, 1.42×10^{15} cm^{-3} and 5.24×10^{15} cm^{-3}, respectively. These materials were chosen to ensure the electronic properties were as close to uniform as possible. All wafers were pyramid textured with a weight loss of 0.46 g (about 4 μm per side). The Cz Si PERC solar cells were finished according to the production line process. An emitter with sheet resistance of 130 Ω/sq was formed by single-side diffusion in a $POCl_3$ tube furnace with two wafers face-to-face in one slot of the process boat. The passivation layer of AlO_x and SiN_x:H layer were successively deposited in a linear remote microwave plasma chemical vapor deposition system (MAiA system, Meyer Burger) at the temperature of 450 °C. Before deposition of the SiN_x:H layers, 18 nm of the AlO_x layer were deposited on the back side of the wafers, and then passivated anti-reflectance layers of SiN_x:H with a thickness of 78 nm and a refractive index of 2.1 at 630 nm were deposited on both sides of the wafers. After laser contact opening and screen printing the front and back sides of the metal contact paste, the wafers were fired at a peak temperature of 880 °C at a belt speed of 6 m/min in a commercial infrared fast–firing furnace. The initial efficiencies of the prepared PERC solar cells were in the range of 20.2%–20.6%.

Accelerated regeneration of LeTID defects was tested using an LED-based light soaking system, which had the capability for light soaking at up to 7 suns intensity and up to 450 °C in device temperatures. Some samples were annealed using RTP instruments at different plateau temperatures. The solar cells were taken out for a light current-voltage (I–V) test at fixed annealing time intervals of 1~20 min. The temperature of the sample in and out of the RTP cavity was set to be 50 °C lower than the annealing temperature, and the heating and cooling rates were fixed so that the two processes took less than 10 s to complete in order to minimize the extra thermal budget effect caused by multiple rounds of heating and cooling of the same sample. In order to test the stability of the treated samples, the regenerated and annealed solar cells were placed on a hot plate and then subjected to light soaking at 75 °C under an LED white light source with an incident irradiance of 1 kW/m^2. During these experiments, the solar cells were taken out for light current-voltage (I–V) tests at varying time intervals. For example in the experiment of light soaking regeneration, the I–V measurement was carried out every 5 s for the first 5 min and every 60 s thereafter. The light I–V parameters of the solar cells were measured with a SINUS-220 LED solar simulator (WAVELABS) under standard test conditions (AM 1.5G spectrum, 1 kW/m^2, 25 °C). It was found during the test that the efficiency decreased as the light I–V test number increased and then tended to stabilize as the test number increased to 10. Therefore, in this study, we recorded the results for every measurement from the 10 continuous tests and denoted the average electric parameter as the final data point. Light soaking was carried out for a maximum of 120 h. To show the evolution of the parameters of the solar cells during the light soaking or the RTP, the measured data for the short-circuit current (I_{sc}), open-circuit voltage (V_{oc}), fill factor (FF), and efficiency were normalized according to the initial value. The collected data were afterwards evaluated using the two-diode model to extract the saturation current density, J_{01} and J_{02} from the first and second diode derived from Suns-V_{oc} measurements.

3. Results and discussions

3.1. Accelerated regeneration through high irradiance at high temperature

In order to observe the dependence of LeTID defect formation and mitigation on B–Ga co-doped cast-mono Si PERC solar cells, Groups A and B were processed at temperatures from 150 °C to 250 °C under a range of illumination intensities. The behavior of the degradation and regeneration of Group A is shown in Fig. 1(a–d). J_{sc} showed comparable changes to V_{oc}, and they had essentially the same change tendency in efficiency, while the FF was not significantly affected. For all samples,

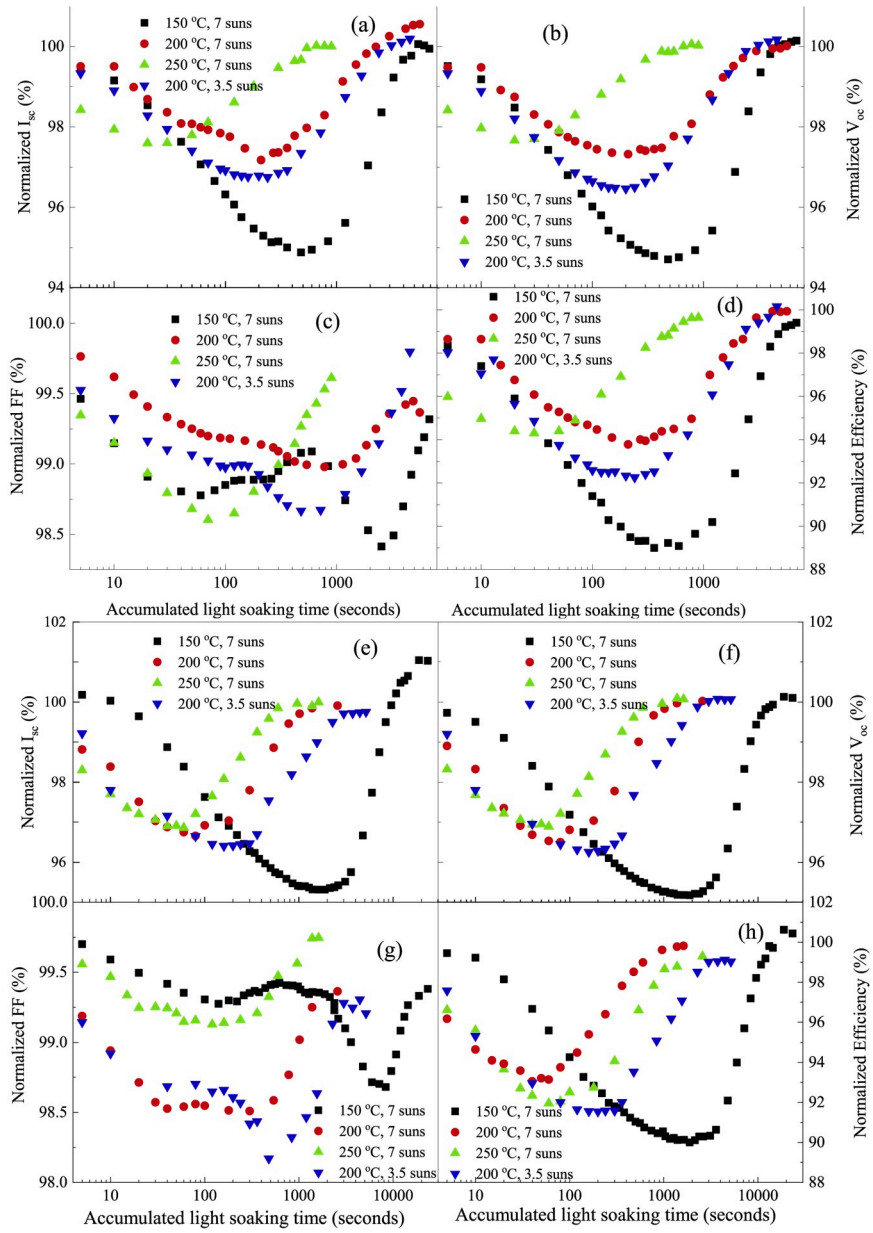

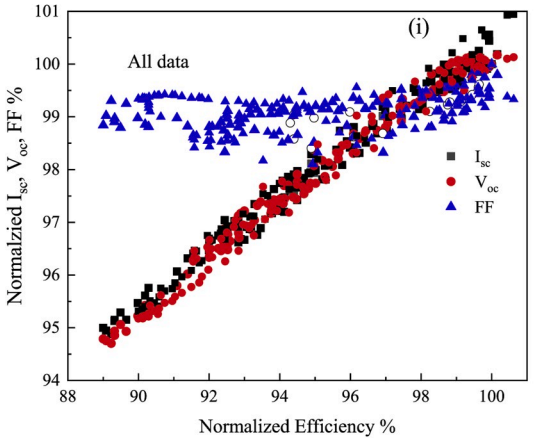

Fig. 1. Normalized I_{sc} (a, e), V_{oc} (b, f), FF (c, g) and efficiency (d, h) *vs* the illumination time at different light intensity and temperature: at 150 °C with 7 suns (black square), at 200 °C with 7 suns (red cycle), at 250 °C with 7 suns (green up-pointing triangle), at 200 °C with 3.5 suns (blue down-pointing triangle). a∼ d: data from Group A; e ∼ h: data from Group B. (i) The normalized V_{oc}, J_{sc} and FF as a function of normalized efficiency from all data from (a)–(i). (For interpretation of the references to colour in this figure legend, the reader is referred to the Web version of this article.)

the degradation and regeneration cycle occurred for four electrical parameters while the ratio of degradation varied. Unlike the other three parameters I_{sc}, V_{oc}, and efficiency, normalized FF presented two degradation curves except when the light soaking was conducted at 250 °C. A clear trend in the higher temperature was observed, resulting in a lower degradation ratio in I_{sc}, V_{oc}, and efficiency. For example, the degradation ratio of V_{oc} decreased from 5% to 2% as the sample temperature increased from 150 °C to 250 °C, and a similar change was observed in I_{sc}. The maximum degradation ratio was only approximately 1.4%–1.6% for FF. The degradation ratio in efficiency varied from 11% to 6% as the temperature changed from 150 °C to 250 °C. Additionally, the I_{sc}, V_{oc}, and efficiency for all samples was able to recover but the recovery time depended on the light soaking temperature, such that the full regeneration time was 600 s and 4000 s for temperatures of 250 °C and 150 °C, respectively. The time it took for the entire degradation and recovery cycle decreased with increasing temperatures due to accelerated reaction rates. There was little difference in the degradation and regeneration time between the results of samples soaked with light intensities of 3.5 suns and 7 suns, while the lower light intensity induced higher degradation ratios. For Group B (Fig. 1(e–h)), I_{sc} and V_{oc} had lower degradation ratios at higher temperatures, and FF had the least degradation in these samples, similar to the results in Group A. The defect kinetics changed between the two groups when the light soaking was at 150 °C with a light intensity of 7 suns: the time when the maximum degradation ratio occurred changed to 500 s for Group A and 1100 s for Group B. However, with the increase in the light soaking temperature and light intensity, the time difference became low and even negligible. The maximum degradation ratio of efficiency for Group B was very close to that of Group A, and the difference was in the range of 0.5–1%. While the maximum degradation ratio of efficiency decreased with increasing temperature and irradiation intensity in Group A, the maximum degradation rate of efficiency in Group B increased with the temperature and intensity (if we exclude the interference of maximum degradation of FF for the sample regenerated at 250 °C). And more, compared to the FF evolution in Group A, the contrast between the two degradations becomes more pronounced.

To clarify the impact of I_{sc}, V_{oc}, and FF on efficiency during the high light intensity soaking at high temperature, a plot of efficiency versus I_{sc}, V_{oc}, and FF is shown in Fig. 1(i). V_{oc} and I_{sc} had a positive linear connection with efficiency. However, FF maintained 99% ± 0.5% of its initial value in the normalized efficiency range of 89%–98%, and in the higher efficiency range, the normalized FF presented slight increases in efficiency. This differed from I_{sc} and V_{oc}, which were mainly influenced by the bulk and surface carrier lifetime (J_{01}). FF was not only affected by the carrier lifetime but also affected by other factors such as series and parallel resistance.

The change tendencies of R_{se} and R_{sh} (not pictured) were not consistent with the change tendency of FF because the series resistance only rose by 15% after 10 s and then was stable, and R_{sh} decreased approximately 10%. To understand the LeTID of the FF, the series resistance and shunt resistance influence on FF was isolated by simulating I–V characteristics using the equivalent circuit model. As R_{se} increased by 15% and R_p decreased by 10%, the simulation result was a loss of 0.4% and almost zero in the FF, demonstrating that the source of the FF degradation and regeneration was not the series resistance and shunt resistance.

The illumination and temperature dependencies for degradation and regeneration characteristics were further examined in relation to J_{01} and J_{02}. J_{01} contributed to the recombination of the base and emitter, including their surfaces, and the second diode current J_{02} was due to recombination within the depletion region. As shown in Fig. 2, the effect of degradation and regeneration was clearly observed in J_{01}. J_{01} showed that the maximum degradation was due to changes in temperature and illumination intensity. J_{01} could represent the parameters of V_{oc} and J_{sc} because they had a corresponding relationship. For example, J_{01} increased as V_{oc} and J_{sc} decreased, and vice versa. The effect of

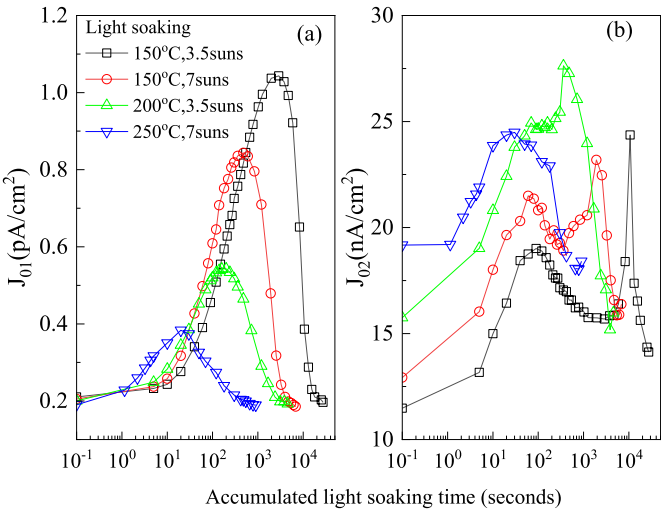

Fig. 2. Degradation and regeneration of the saturation current density J_{01} (a) and J_{02} (b) derived from the 2-diode model for Group A under illumination at elevated temperatures.

temperature and light intensity on degradation ratio and degradation time was similar to the effect on V_{oc} and J_{sc}, in which there was faster degradation and regeneration, and less degradation under higher temperatures and higher light intensity. As discussed in the previous section (Fig. 1), as samples were exposed to a light soaking temperature below 250 °C or an intensity of light lower than that of 3.5 suns, two degradation-regeneration cycles were observed in the FF. As seen in Figs. 1(c), (g) and 2(b), the time dependences of FF and J_{02} were identical; therefore it was concluded that J_{02} dominated the FF in the full degradation and regeneration cycles. It was notable that the first J_{02} peak occurred at a shorter light soaking time that was almost independent of temperature and light intensity, but the second largest peak position occurred in less time as the temperature and light intensity increased.

The underlying physical mechanisms for the first degradation-regeneration cycle of J_{02} are still unclear but there may be two explanations. One is the boron-oxygen defect formation and passivation. The boron–oxygen complex may result in a strongly increased dark current in the depletion region due to a strong injection level dependence on the carrier lifetime [22]. Another possibility is that the intrinsic defects have a more influence on J_{02}, such as the dislocations or grain boundary. These defects may induce higher dark current in the depletion region and have more influence on J_{02} than J_{01}. A single degradation–regeneration cycle in J_{01} implied that the effect of LeTID defects exceeded that of the boron–oxygen complex on carrier recombination. The second J_{02} peak was contributed to by the LeTID defect formation. The time it took to get the second J_{02} maximum was always after that of J_{01} in all the samples. This indicated that the reaction rate of the LeTID defect in the depletion region was slower than that in neutral regions, such as in the emitter and base. When temperatures were higher, the reaction rate for LeTID was fast enough to overtake the first defect reaction, so it reached one peak when the temperature reached up to 250 °C.

A single step increase and decrease was observed in J_{01}; thus, an exponential function with one growth phase and one decay phase was carried out for the full curves in all samples (as shown in Fig. 3(a)) to extract the degradation and regeneration time constant with the J_{01} fitting. To determine the active energy used in the formation of the defect, Fig. 3(b) shows an Arrhenius plot of the defect formation and regeneration rate (1/time constant) as a function of the inverse temperature (1000/T) using the formula:

$$\frac{1}{time\ condtant} = A\exp\left(-\frac{E_a}{K_B T}\right)$$

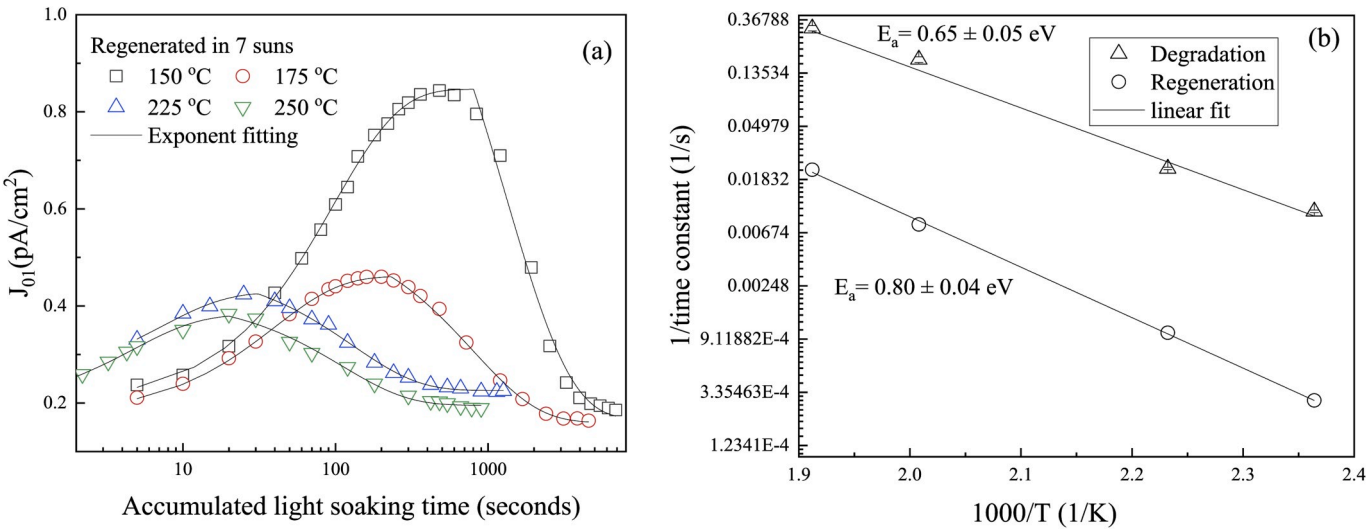

Fig. 3. Fit parameters: (a) Evolution of the saturation current density J_{01} derived from the 2-diode model for Group A light soaked with the illumination intensity of 7 kW/m^2 at different temperature, the solid lines represent double exponential decay fits to the data. (b) Arrhenius correlation between temperature and degradation/regeneration rate, the lines correspond to a fit to the Arrhenius analysis, gives thermal activation energy of 0.65 eV and 0.80 eV, respectively.

Where 1/time constant and A, K_B, T, E_a correspond to the defect reaction rate, exponential temperature independent pre-factor, Boltzmann's constant, and temperature and reaction activation energy, respectively. The Arrhenius activation energies for the defects in the degradation and regeneration stages were 0.65 ± 0.05 eV and 0.80 ± 0.04 eV, respectively. These values were close to the reported values of 0.62–0.78 eV and 0.67–0.78 eV for the mc-Si lifetime samples in which the illumination condition used was higher by 2–10 times [10] than was used in this work. Vargas Carlos reported activation energy of 1.08 ± 0.05 eV for the degradation process and 1.11 ± 0.04 eV for the regeneration process in mc-Si lifetime wafers under dark annealing [23]. This activation energy was significantly higher than the values measured in this work. One possible reason for this is that the recombination enhanced defect reactions to reduce the activation energy needed under high injection levels. However, all of the reference values came from the lifetime sample; more values from p-type mc-Si PERC solar or cast-mono Si PERC solar cells are needed to be compared in the future.

A stability test was conducted on the regenerated solar cells under the conditions of illumination with 1 sun at 75 °C for 120 h. The results are shown in Fig. 4. In Group A, all solar cells showed degradation, with a higher sensitivity than the as-prepared PERC solar cells (degradation ratio of 3.5% at 20 h), and lower sensitivity than the regenerated PERC solar cells (degradation ratio of 0–1.5% at 20 h). This revealed that the treated cells were substantially more stable than the untreated controls. The degradation extent in untreated Group A was 2.5% and 3.5%, whereas it was 6% and 8% in untreated Group B for 5 h and 20 h (not shown in Fig. 4), respectively. The degradation of the as-prepared PERC solar cell was less severe compared to the results from the Boron doped mono-like PERC solar cells with an average relative degradation of 9.1% after 5 h of light soaking at 65 °C under an irradiance level of 1 sun [17]. A possible explanation for this is the different effects of B versus Ga doping, but different impurity concentrations may also be the reason due to the different silicon manufacturers.

The solar cell regenerated at 200 °C with a light intensity of 7 suns showed a slight decline, and maximum degradation was observed after 80 h, after which it began to recover. In the other samples, there was an increase in efficiency within the first 20 h, but as the LeTID time

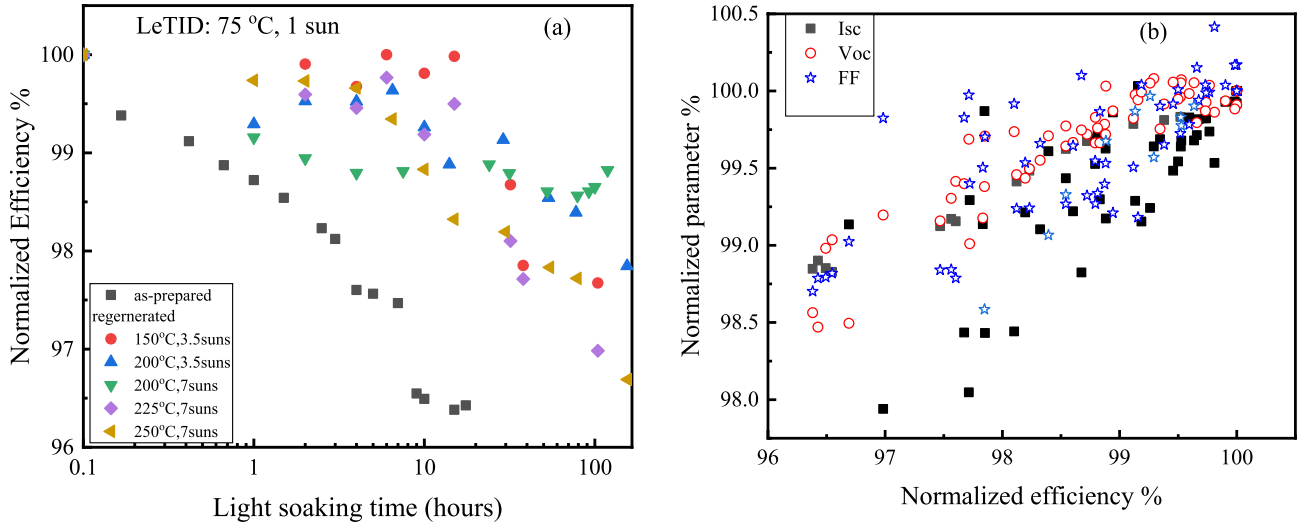

Figure 4. Presents the result of stability test at the 75 °C with 1 kW/m^2 illumination for Group A regenerated at different temperature at the light intensity of 7 suns (7 kW/m^2), regenerated at 200 °C with light intensity of 3.5 suns (3.5 kW/m^2); as-prepared solar cells as reference. (a) The time dependence of normalized efficiency of the regenerated PERC solar cells during the subsequent 150 h stability test. (b) The normalized V_{oc}, J_{sc} and FF as a function of normalized efficiency from (a).

extended, there was continual degradation indicating that further testing would lead to more degradation. Therefore, in this LeTID test time range, the best regeneration condition was light soaking at 200 °C with a light intensity of 7 kW/m^2. The effective minority carrier lifetime of the as-fired lifetime samples in the two groups (the semi-finished solar cell) decreased continuously for 500 h, and then slowly began to recover during the stability test. The lifetime recovered and stabilized after 200 h when the samples regenerated to the best condition (in press). The maximum degradation ratio was 12% and 80% for the samples regenerated to the best condition and the as-fired lifetime sample, respectively. Compared to the as-prepared PERC solar cells, the accelerated degradation/recovery process is significantly benefited to suppress degradation in the subsequent LeTID test. As shown in Fig. 4(b), in the test time range of 120 h, I_{sc}, V_{oc}, and FF almost had similar ranges in degradation ratios, and all of them had a linear relation with efficiency. However, based on the results of the light soaking regeneration (as shown in Fig. 1(e)), the efficiency degradation and regeneration mainly contributed to V_{oc} and I_{sc}, while FF had the least change in the full process. This difference may be due to the bulk carrier lifetime influence, in other words, the passivated bulk recombination-active defect that formed during the light soaking regeneration had a slight effect on the bulk carrier lifetime during the stability test.

As seen in Fig. 1, the variation in the degradation ratio and time for the samples that were regenerated at different temperatures resulted from the different thermal activation energy of the degradation (E_a ~0.65 eV) and regeneration (E_a ~0.80 eV). At higher temperatures, the regeneration transformed the generated harmful defects more quickly; this may have left some number of harmful defect precursors to not get fully degraded in the bulk. However, when the temperature was lower, the defects from LeTID may not have been fully regenerated. An incomplete LeTID defects formation and regeneration eliminated only part of the harmful defects and thus led to a reduced but still observable degradation, as shown in Fig. 4, where the samples regenerated at lower temperatures of 150 °C and higher temperatures of 250 °C.

3.2. Impact of a flash light on the instability of Si solar cells during I–V test

During the light I–V test, the electrical parameters were not stable. As shown in Fig. 5, I_{sc} and FF decreased initially with the increase in the light I–V test number and they tended to be stable until the flash number was in the dozens, though V_{oc} generally increased continuously. In order to analyze this change, we calculated the ratio of the average value of 10 tests to the value of the first test (initial value). If the normalized ratio was always close to 100%, it meant that the electric parameter was almost stable under multi I–V tests. The relative changes in V_{oc}, I_{sc}, and FF were very small, and the efficiency only decreased 0.5% from the first test to the 10th test. Fig. 6 plots the ratio between the average value of multiple tests and the value of the first test with the illumination time for samples regenerated at 200 °C with a light intensity of 7 kW/m^2; the average V_{oc} and I_{sc} values plotted as a function of light soaking time are shown in the insert. There was a close connection between the normalized ratio and the value of I_{sc} and V_{oc}. First, in the degradation stage, the ratio between the average value and the first test value gradually closed to 100%. This indicated that the defects related to this change were gradually reduced by transforming into other defects or by H passivation. Second, in the regeneration stage, the ratio gradually moved away from 100% with the extension of light soaking time, indicating that the defect concentration was gradually increasing. This normalized ratio was close or equal to 100% earlier than it took for I_{SC} and V_{OC} to reach the maximum degradation ratio. After it got close or equal to 100%, it was stable for a period of time and then increased or decreased until I_{sc} or V_{oc} began to recover. Furthermore, the degradation ratio of performance induced by this instability during the I–V test (0.5%) was far lower than the value of the LeTID-induced performance degradation (about 6%). This may imply that the defect-induced instability in the solar cell's performance under the light I–V test was not the LeTID defect, but was involved in the degradation and regeneration reaction.

This instability of Si solar cells during the light flash at room temperature has been attributed to iron-boron dissociation in P-type mc-Si solar cells [24]. The Fe–Ga can be optically dissociated similar to Fe–B pairs. Furthermore, the difference in recombination activity between Fe–B and Fe_i is similar to that between Fe–Ga and Fe_i in terms of injection-dependent carrier lifetime [25]. Therefore, though there is a small quantity of Ga dopant in the cast-mono Si PERC solar cells, in this work we only used the Fe–B as a representative. The injection level dependence of the corresponding carrier lifetimes was much more pronounced for isolated Fe_i than for Fe–B pairs, and their injection-dependent lifetime curves crossed at an approximately fixed excess carrier concentration below 1×10^{14}/cm^3 [26]. Above this point, the SRH lifetime from Fe_i was higher than that from Fe–B; otherwise, it was the opposite. The different positions along the I–V-curve corresponded to different excess carrier injection levels. I_{sc} and FF dominated at the low excess carrier injection levels. When the defect shifted from Fe–B to Fe_i, I_{sc} and FF began to degrade due to the increasing SRH

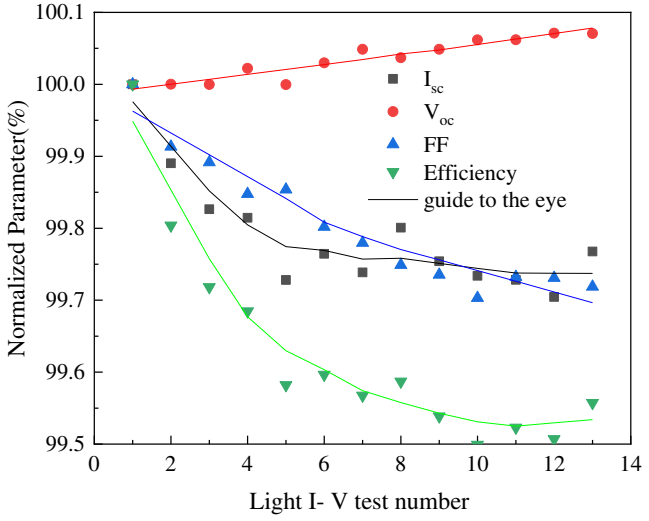

Fig. 5. Normalized parameters of V_{oc}, I_{sc}, FF and efficiency as a function of light I–V number. The straight line is just for guiding to the eye. The result was from the as-prepared Group A.

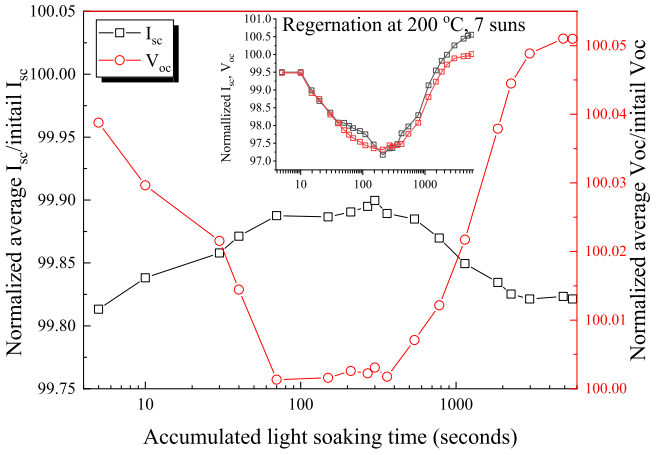

Fig. 6. Normalized ratio of average V_{oc} and I_{sc} for light I–V test 10 times to the initial value (the first test) vs the light soaking time. (a) Samples regenerated at 200 °C with light intensity of 7 kW/m^2, the insert shows the function of normalized V_{oc} and I_{sc} with the accumulated light soaking time.

dependence. While V_{oc} worked at the high injection level (high excess carrier concentration, ~10^{15}/cm^3), it increased if the Fe–B pair dissociated from Fe_i.

In the literature, B–O defects or iron-boron (Fe–B) pairs have been excluded as possible defect candidates for LeTID in Si PERC solar cells [27]. However, in that case, what is the role of the Fe–B pair in the full degradation-regeneration cycle? One possibility is that, in the stage of degradation, the dissociation of B–H and Ga–H complexes offer sufficient H atoms [28] for H passivation of Fe–B and Fe–Ga pairs, or Fe_i [29] in the hydrogenation process at elevated temperatures with high-intensity illumination. With further illumination and heating occurring, the bond broke and released hydrogen, passivating the defects from LeTID, and thus the defects from Fe–B appeared in the bulk (regeneration stage). Fe–B was not a defect precursor or defect in the LeTID process, but did react with hydrogen during the process, which affected the kinetic behavior of hydrogen.

3.3. The impact of RTP treatment on the evolution of solar cell efficiency and LeTID mitigation

The finished PERC solar cells were annealed using RTP in order to investigate the effect of the annealing temperature on solar cells efficiency and stability in the LeTID test for Group B. Fig. 7 shows the normalized I_{sc}, V_{oc}, FF, and efficiency based on annealing time at temperatures of 250 °C, 300 °C, and 350 °C. At the temperatures of 250 °C and 300 °C, an evident degradation and regeneration cycle was observed. Similar degradation and lifetime recovery due to dark annealing of B-doped Cz and mc-Si wafers was observed [30]. The sample treated at 300 °C reached the maximum degradation after only 2 min and then quickly rose to over 100% in value in the span of 20 min. However, after annealing at 250 °C for 50 min, it did not recover to the initial value and stabilized at 98.2% of the initial efficiency. The light illumination helped to speed the degradation and increase the degradation ratio, which was the same in the regeneration process if the samples were heated at the same temperature (compared to the result in Fig. 1). Above 300 °C, no degradation was observed and an improvement in performance was immediately observed within 12 min, but if the time extended beyond that, the FF began to decrease because of an increase in series resistance, possibly due to the metal contact penetrating further into the Si wafer. If the RTP temperature was higher, such as 400 °C or 450 °C, the V_{oc}, I_{sc}, FF, and efficiency increased. However, the FF decreased by 20% when the annealing time was 2 min. The increase in V_{oc}, I_{sc}, and FF may have contributed to the dissociation or slow hydrogen passivation of other SRH-related recombination components in the bulk, such as metal impurities and crystallographic defects [31].

The stability test results for RTP were treated at temperatures of 350 °C for 12 min and 450 °C for 1 min, as compared to an accelerated regeneration at 150 °C–225 °C with a light intensity of 7 kW/m^2. The as-prepared PERC solar cells are shown in Fig. 8. The efficiency continued to degrade and did not reach the maximum degradation point in the range of 120 h for all samples, and the as-prepared solar cell had the highest degradation ratio. It was expected that the RTP treatment would increase the stability because of the decreasing defect concentration or passivating defect after RTP treatment at higher temperatures as evidenced by the rise in I_{sc}, V_{oc}, FF, and efficiency. However, the results of

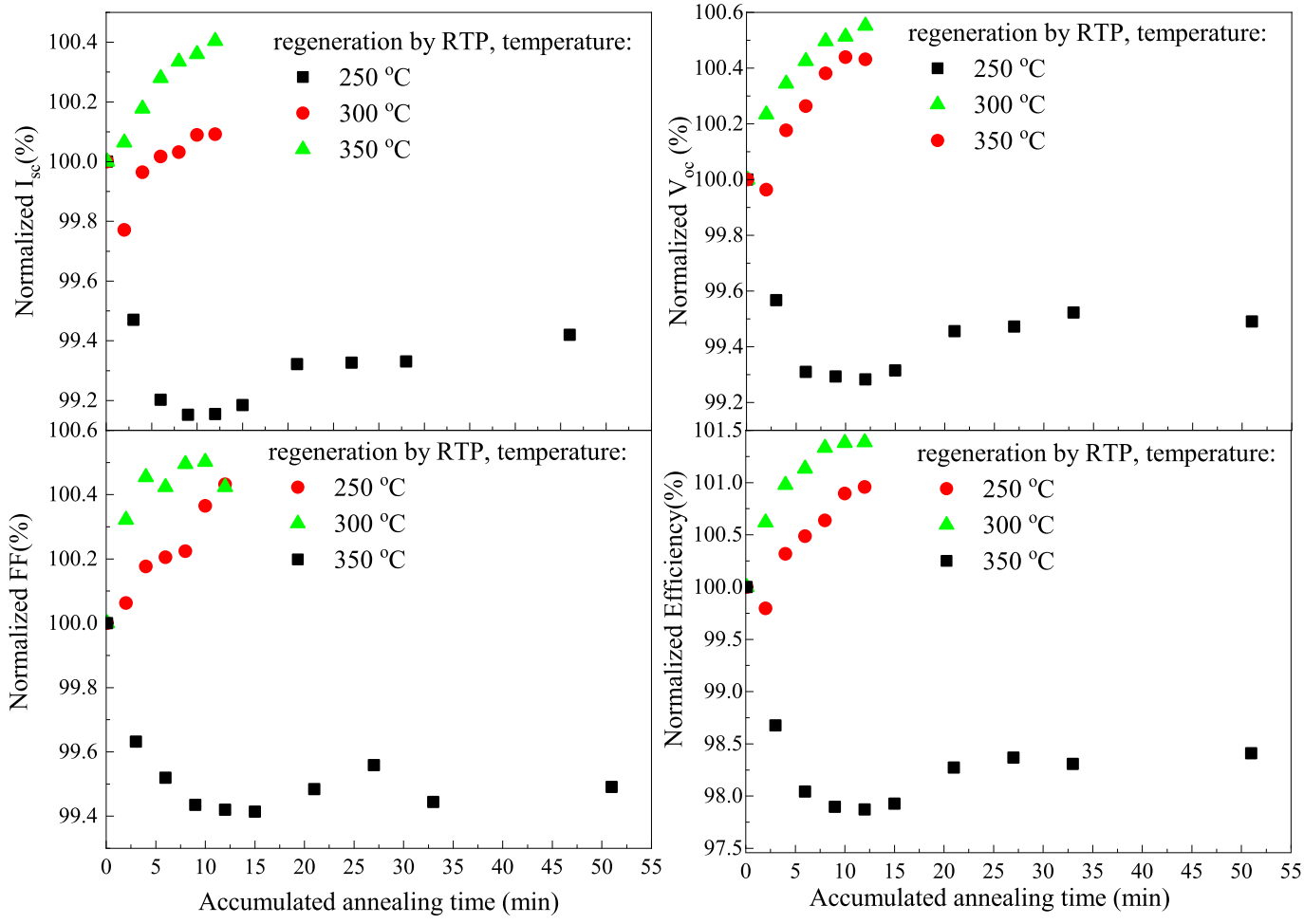

Fig. 7. Evolution of the normalized I_{sc}, V_{oc}, FF and efficiency during the RTP annealing process at different temperature. The result was from Group B.

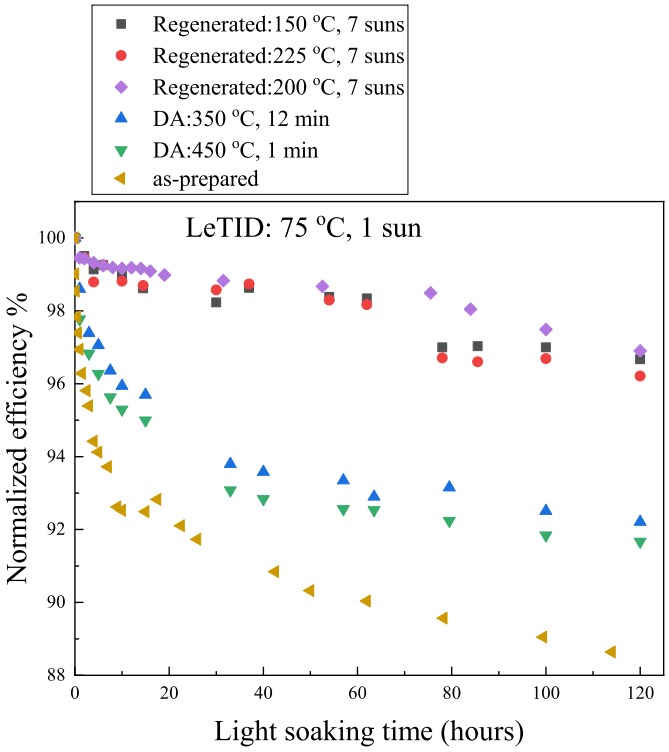

Fig. 8. Progress of normalized efficiency change during LeTID test at 75 °C with 1 sun for regenerated Group B by RTP annealing and light soaking with high light intensity, as-prepared solar cells as reference.

the LeTID stability test under the conditions of 75 °C with an illumination intensity of 1 kW/m^2 showed that this was not the case. The RTP treated samples presented more severe degradation than the regenerated cells that were treated by high irradiation at elevated temperatures during the post-LeTID stability test, even though this RTP treatment helped to suppress the LeTID degradation compared to the as-fired solar cells. In the range of 120 h, the maximum efficiency degradation for the as-prepared samples was 12%, whilst for the samples using light soaking accelerated to the best condition and RTP treated at 350 °C for 12 min, the maximum efficiency degradation was 3.5% and 8%, respectively. Thus, the maximum efficiency degradation was suppressed by approximately 70% and 30%, respectively. This implies that the RTP treatment slightly suppressed the degradation of cast-mono p-type Si PERC solar cells during the LeTID stability test even though this process could have improved the efficiency of the solar cells if the appropriate RTP temperature and time was used. Similar results have been reported in Tabea's result that showed, even after recovery, the dark anneal at 175 °C did not yield LeTID stable mc-Si PERC solar cells [32]. Vargas et al. also observed an improvement in the lifetime of mc-Si when the annealing temperature was 300 °C, but this improvement was not stable under light soaking at elevated temperatures [23]. It is possible that a portion of the observed efficiency improvement was associated with the recovery of pre-existing LeTID-related defect precursors formed during the firing treatment as suggested by Chen et al. [30]. The lowest degradation ratio of 3% was observed in the samples regenerated at 200 °C with a light intensity of 7 kW/m^2. It showed that the best accelerated regeneration condition from illumination with high light intensity and at elevated temperatures was the same for Group A and Group B. However, the degradation ratio for cells regenerated to the best condition and as-prepared in Group B was 2%, and 7.5% higher than that in Group A after a stability test of 120 h and 20 h, respectively. This indicated that the lower interstices oxygen concentration in Si bulk had a positive effect on suppressing LeTID behavior.

In summary, with a light intensity of 7 kW/m^2, the 200 °C treatment proved to be the most promising, resulting in only a small degradation of the other treated samples during the 120 h-long stability test. Limited by the maximum intensity of 7 kW/m^2 in this system, the best condition treated samples still showed a certain degree of degradation due to LeTID, suggesting that further study of the effect of illumination intensity is needed in order to achieve complete stability. It is hypothesized that the RTP pre-accelerated regeneration step may provide both the improved performance and high anti-LeTID properties in Si PERC solar cells, but this effect needs be verified further.

4. Conclusion

In this work, a fast regeneration process was applied to Ga–B co-doped cast mono Si PERC solar cells in order to investigate the defect kinetics at high illumination intensities and varying temperatures. The tests showed that the degradation and regeneration of electrical parameters of the solar cells had a clear dependence on the sample temperature and light intensity during illumination. The activation energies for the defect formation and migration were 0.65 ± 0.05 eV and 0.80 ± 0.04 eV, respectively. It was notable that the Fe–B and Fe–Ga pairs decreased the efficiency initially, but then almost stabilized during the light I–V test. These defects were not all defect precursors or defects from degradation, but they could all react with hydrogen during the degradation-regeneration process. The stability of the regenerated solar cells was observed under the LeTID test condition, which was light soaking at 75 °C and a light intensity of 1 kW/m^2. The regeneration condition of 200 °C and illumination intensity of 7 kW/m^2 supported the best anti-LeTID performance. When samples were annealing in the RTP instrument at temperatures of 250 °C and 300 °C, a full curve from degradation to regeneration cycle was observed. For temperatures above 300 °C, no obvious degradation was observed, but there was an improvement in performance. These annealed PERC solar cells had more severe degradation than those with accelerated regeneration by high irradiation at elevated temperatures even though they had slight improvements in anti-LeTID effects compared to as-prepared solar cells during the stability test under the conditions of 75 °C with an illumination intensity of 1 kW/m^2. It demonstrates the application of a fast (around 20 min) regeneration method could be coupled in mass production. Limited by the maximum intensity of 7 kW/m^2 in this system, the best condition treated samples still showed a certain degree of degradation due to LeTID, suggesting that further study of the effect of illumination intensity is needed in order to achieve complete stability. Further, RTP treatment combining with accelerated regeneration step may be a potential method to provide both the improved performance and high anti-LeTID properties in Si PERC solar cells.

Declaration of competing interest

The authors declare that they have no known competing financial interests or personal relationships that could have appeared to influence the work reported in this paper.

CRediT authorship contribution statement

Chunlan Zhou: Conceptualization, Methodology, Investigation, Writing - review & editing. **Fangxu Ji:** Formal analysis. **Shangzhi Cheng:** Formal analysis. **Junjie Zhu:** Resources. **Wenjing Wang:** Project administration. **Dongli Hu:** Resources.

Acknowledgments

This work has been supported by grants from the National Key R&D Program of China (Grant No.2018YFB1500303), the National Natural Science Foundation of China (Grant No.61874120), State Administration of Foreign Experts Affairs (Overseas Training project: P193041032), and by Norwegian Research Council (project 261574 and

280909).

Appendix A. Supplementary data

Supplementary data to this article can be found online at https://doi.org/10.1016/j.solmat.2020.110508.

References

[1] N.E. Grant, J.R. Scowcroft, A.I. Pointon, M. Al-Amin, P.P. Altermatt, J.D. Murphy, Lifetime instabilities in gallium doped monocrystalline PERC silicon solar cells, Solar Energy Materials and Solar Cells. https://doi.org/10.1016/j.solmat.2019.110299, 2019.

[2] Friederi keKersten, P. Engelhart, H.-C. Ploigt, A. Stekolnikov, T. Lindner, F. Stenzel, M. Bartzsch, A. Szpeth, K. Petter, J. Heitmann, J.W. Müller, Degradation of multicrystalline silicon solar cells and modules after illumination at elevated temperature, Sol. Energy Mater. Sol. Cells 142 (2015) 83–86, https://doi.org/10.1016/j.solmat.2015.06.015.

[3] Friederike Kersten, F. Fertig, K. Petter, B. Klöter, E. Herzog, M.B. Strobel, J. Heitmann, Jörg W. Müller, System performance loss due to LeTID, Energy Procedia 124 (2017) 540–546, https://doi.org/10.1016/j.egypro.2017.09.260.

[4] Annika Zuschlag, D. Skorka, G. Hahn, Degradation and regeneration in mc-Si after different gettering steps, Prog. Photovoltaics Res. Appl. 25 (2017) 545–552, https://doi.org/10.1002/pip.2832.

[5] Wolfram Kwapila, Tim Niewelt, M.C. Schubert, Kinetics of carrier-induced degradation at elevated temperature inmulticrystalline silicon solar cells, Sol. Energy Mater. Sol. Cell. 173 (2017) 80–84, https://doi.org/10.1016/j.solmat.2017.05.066.

[6] C. Chan, T.H. Fung, M. Abbott, D. Payne, A. Wenham, B. Hallam, R. Chen, S. Wenham, Modulation of carrier-induced defect kinetics in multi-crystalline silicon PERC cells through dark annealing, Sol. RRL 1 (2017), 1600028, https://doi.org/10.1002/solr.201600028.

[7] D. Bredemeier, D. Walter, J. Schmidt, Light-induced lifetime degradation in high-performance multicrystalline silicon: detailed kinetics of the defect activation, Sol. Energy Mater. Sol. Cell. 173 (2017) 2–5, https://doi.org/10.1016/j.solmat.2017.08.007.

[8] Friederike Kersten, P. Engelhart, H.-C. Ploigt, A. Stekolnikov, T. Lindn, A new mc-Si degradation effect called LeTID, in: IEEE 42nd Photovoltaic Specialist Conference (PVSC); New Orleans, LA, USA2015, 2015, pp. 1–5, https://doi.org/10.1109/PVSC.2015.7355684.

[9] David N.R. Payne, C.E. Chan, B.J. Hallam, B. Hoex, M.D. Abbott, S.R. Wenham, D. M. Bagnall, Rapid passivation of carrier-induced defects in p-type multi-crystalline silicon, Sol. Energy Mater. Sol. Cell. 158 (2016) 102–106, https://doi.org/10.1016/j.solmat.2016.05.022.

[10] S. Liu, C. Chan, D. Chen, M. Kim, C. Sen, U. Varshney, B. Hallam, M. Abbott, S. Wenham, D. Payne, Investigation of temperature and illumination dependencies of carrier-induced degradation in p-type multi-crystalline silicon, AIP Conf. Proc. 1999 (2018), 130014, https://doi.org/10.1063/1.5049333(2018)130014.

[11] J. Shao, X. Xi, S. Li, G. Liu, R. Peng, C. Li, G. Chen, R. Chen, Longer hydrogenation duration for large area multi-crystalline silicon solar cells based on high-intensity infrared LEDs, Optic Commun. 450 (2019) 252–260, https://doi.org/10.1016/j.optcom.2019.06.011.

[12] L. Helmich, D.C. Walter, D. Bredemeier, R. Falster, V.V. Voronkov, J. Schmidt, In-situ characterization of electron-assisted regeneration of Cz-Si solar cells, Sol. Energy Mater. Sol. Cell. 185 (2018) 283–286, https://doi.org/10.1016/j.solmat.2018.05.023.

[13] Catherine E. Chan, David N.R. Payne, Brett J. Hallam, Malcolm D. Abbott, Tsun H. Fung, Alison M. Wenham, S. Budi, Tjahjono, S.R. Wenham, Rapid stabilization of high-performance multicrystalline P-type silicon PERC cells, IEEE J. Photovolt. 6 (2016) 1473–1479, https://doi.org/10.1109/JPHOTOV.2016.2606704.

[14] Chandany Sen, C. Catherine, H. Phillip, W. Matthew, V. Utkarshaa, L. Shaoyang, C. Daniel, S. Aref, C. Alison, C. CheeMun, H. Brett, A. Malcolm, Annealing prior to contact firing: a potential new approach to suppress LeTID, Sol. Energy Mater. Sol. Cell. 200 (2019) 109938, https://doi.org/10.1016/j.solmat.2019.109938.

[15] M. Yli-Koski, M. Serué, C. Modanese, H. Vahlman, H. Savin, Low-temperature dark anneal as pre-treatment for LeTID in multicrystalline silicon, Sol. Energy Mater. Sol. Cell. 192 (2019) 134–139, https://doi.org/10.1016/j.solmat.2018.12.021.

[16] T. Niewelt, M. Selinger, N.E. Grant, W. Kwapil, J.D. Murphy, M.C. Schubert, Light-induced activation and deactivation of bulk defects in boron-doped float-zone silicon, J. Appl. Phys. 121 (2017), 185702, https://doi.org/10.1063/1.4983024.

[17] H.C. Sio, H. Wang, Q. Wang, C. Sun, W. Chen, H. Jin, D. Macdonald, Light and elevated temperature induced degradation in p-type and n-type cast-grown multicrystalline and mono-like silicon, Sol. Energy Mater. Sol. Cell. 182 (2018) 98–104, https://doi.org/10.1016/j.solmat.2018.03.002.

[18] S. Zhang, J. Peng, H. Qian, H. Shen, Q. Wei, W. Lian, Z. Ni, J. Jie, X. Zhang, L. Xie, The impact of thermal treatment on light-induced degradation of multicrystalline silicon PERC solar cell, Energies 12 (2019) 416, https://doi.org/10.3390/en12030416.

[19] T. Isao, J. Supawan, I. Taisho, U. Noritaka, Seed manipulation for artificially controlled defect technique in new growth method for quasi-monocrystalline Si ingot based on casting, Appl. Phys. Exp. 8 (2015), 105501, https://doi.org/10.7567/APEX.8.105501.

[20] Xiong Zheng, Chunlan Zhou, Xiaojie Jia, Endong Jia, Wenjing Wang, Deep-level transient spectroscopy characterization of electrical traps in p-type multicrystalline silicon with gettering and hydrogenation process, Sol. Energy 162 (2018) 372–377, https://doi.org/10.1063/1.371186.

[21] C.L. Zhou, S. Zhou, F.X. Ji, W.J. Wenjing, Deep level transient spectroscopic investigation of carrier trap defects in p-type mc-Si PERC solar cells after elevated temperature light soaking, in: 36th European Photovoltaic Solar Energy Conference and Exhibition, Marseille, 2019, https://doi.org/10.1016/j.solener.2018.01.027.

[22] J. Schmidt, A. Cuevas, Electronic properties of light induced recombination centers in boron doped Czochralski silicon, J. Appl. Phys. 86 (1999) 3175.

[23] Vargas Carlos, C. Gianluca, C. Catherine, P. David, H. Ziv, On the impact of dark annealing and room temperature illumination on p-type multicrystalline silicon wafers, Sol. Energy Mater. Sol. Cell. 189 (2019) 166–174, https://doi.org/10.1016/j.solmat.2018.09.018.

[24] J. Schmidt, Effect of dissociation of iron-boron pairs in crystalline silicon on solar cell properties, Prog. Photovoltaics Res. Appl. 13 (2005) 325–331, https://doi.org/10.1002/pip.594.

[25] Jan Schmidt, D. Macdonald, Recombination activity of iron-gallium and iron-indium pairs in silicon, J. Appl. Phys. 97 (2005), 113712, https://doi.org/10.1063/1.1929096.

[26] Daniel Macdonald, A. Cuevas, Reduced fill factors in multicrystalline silicon solar cells due to injection-level dependent bulk recombination lifetimes, Prog. Photovoltaics Res. Appl. 8 (2000) 363–375, https://doi.org/10.1002/1099-159X(200007/08)8:4<363::AID-PIP328>3.0.CO;2-Y.

[27] D.N.R. Payne, C.E. Chan, B.J. Hallam, B. Hoex, M.D. Abbott, S.R. Wenham, D. M. Bagnall, Acceleration and mitigation of carrier-induced degradation in p-type multi-crystalline silicon, Phys. Status Solidi Rapid Res. Lett. 10 (2016) 237–241, https://doi.org/10.1002/pssr.201510437.

[28] Daniel Chen, M. Kim, B.V. Stefani, B.J. Hallam, M.D. Abbott, C.E. Chan, R. Chen, D. N.R. Payne, N. Nampalli, A. Ciesla, T.H. Fung, K. Kim, S.R. Wenham, Evidence of an identical firing-activated carrier-induced defect in monocrystalline and multicrystalline silicon, Sol. Energy Mater. Sol. Cell. 172 (2017) 293–300, https://doi.org/10.1016/j.solmat.2017.08.003.

[29] C.H. Seager, R.A. Anderson, Two-step debonding of hydrogen from boron acceptors in silicon, Appl. Phys. Lett. 59 (1991) 585, https://doi.org/10.1063/1.105394.

[30] X. Hou, S. Yuan, X. Yu, X. Zhu, D. Yang, Hydrogen passivation of iron-acceptor pairs in boron and gallium co-doped crystalline silicon, APEX 13 (2020), 011002, https://doi.org/10.7567/1882-0786/ab58e2.

[31] Fung Tsun Hang, M. Kim, D. Chen, A. Samadi, C.E. Chan, B.J. Hallam, S. Wenham, M. Abbott, Influence of bound hydrogen states on carrier-induced degradation in multi-crystalline silicon, AIP Conf. Proc. (1999), 130004, https://doi.org/10.1063/1.5049323, 2018.

[32] Tabea Lukal, M. Turek, C. Hagendorf, Defect formation under high temperature dark-annealing compared to elevated temperature light soaking, Sol. Energy Mater. Sol. Cell. 187 (2018) 194–198, https://doi.org/10.1016/j.solmat.2018.06.043.